Nanotechnology **21** (2010) 105602 (7pp) doi:10.1088/0957-4484/21/10/105602

Size-controlled growth of colloidal gold nanoplates and their high-purity acquisition

X Fan[1,4], Z R Guo[2,4], J M Hong[3], Y Zhang[1], J N Zhang[2] and N Gu[1,5]

[1] State Key Laboratory of Bioelectronics and Jiangsu Key Laboratory for Biomaterials and Devices, Southeast University, Nanjing 210096, People's Republic of China
[2] The Research Institute of Cardiovascular Disease, The First Affiliated Hospital of Nanjing Medical University, Nanjing 210029, People's Republic of China
[3] Modern Centers of Analyses, Nanjing University, Nanjing 210093, People's Republic of China

E-mail: guning@seu.edu.cn

Received 9 December 2009, in final form 12 January 2010
Published 15 February 2010
Online at stacks.iop.org/Nano/21/105602

Abstract
A facile while flexible approach to size-controllable high-purity colloidal gold nanoplates has been presented. By adjusting the quantity of seeds and I^- through a seed-mediated, cetyltrimethylammonium bromide (CTABr)-assisted synthetic system, the edge length of the gold nanoplates can be adjusted from 140 to 30 nm without changing their thickness or crystal structure. By simply increasing the ion concentration of the reaction solution, the as-prepared gold nanoplates can be deposited due to the different electrostatic aggregation effects between nanoplates and spherical nanoparticles. Effective storage methods to keep the structural and optical stability of these gold nanoplates are also proposed.

(Some figures in this article are in colour only in the electronic version)

1. Introduction

Metal nanostructures play important roles in many areas by virtue of their fascinating properties. Their optical properties [1], together with their electrical [2, 3], catalytic [4, 5] properties, etc, are most attractive in gold and silver nanostructures. The optical properties of the nanostructures are strongly dependent on their shape and size [6, 7]. Therefore, there has been an explosion of interest in developing versatile methods for shape-controlled synthesis of these nanostructures for extending their optical properties according to human wishes.

In general, metal nanoplates are a class of single-crystal two-dimensional structures with a nanoscale thickness. The micrometer-sized metal nanoplates with thickness below 100 nm are also regarded as nanoplates, but their optical properties are not as remarkable as their colloidal analogs [8]. Gold and silver nanoplates have been established to hold potential applications in photonics, optical sensing, biological labeling, and near-infrared light absorbing due to their unique optical properties known as localized surface plasmon resonance (SPR) [9–12]. By contrast to silver nanoparticles, gold nanoparticles are more widely used in biomedical fields because of their excellent biocompatibility and non-toxicity [13]. Moreover, gold nanoplates are considered to have potential use in cancer hyperthermia, for the reason that their SPR band can be tuned in the range of the near-infrared region [14, 15]. And similar to other shaped gold nanostructures, gold nanoplates could also hold the ability of targeting malignant tumors with high specificity when conjugated with targeting ligands such as antibodies or small molecules [16, 17].

To date, there have been numerous publications about gold nanoplates. Most of them focused on sub-micrometer- or micrometer-sized plates, where the large size leads to instability in solution phase and loss of colloidal

[4] XF and ZG contributed equally to this work.
[5] Author to whom any correspondence should be addressed.

properties, which further limits their applications in biomedical fields [18–21]. A few other reports covered small gold nanoplates that often generate considerable side products, which are difficult to separate [22, 23]. Moreover, the shape and size of gold nanoplates are not as easy to control as those of silver ones. Recently, Millstone *et al* have reported an approach to control the size of gold nanoplates from beyond 100 nm to larger [24]. However, there are still a large number of spherical nanoparticles existing in the colloidal solution even after purification, and the long-wavelength SPR band which is beyond 1200 nm will be greatly influenced by the intensively near-infrared absorption of water. Low-purity often leads to loss of stability and limits the effects of the gold nanoplates when used in assembly, labeling, sensing, or drug delivery. Moreover, therapeutic strategies have been reported that near-infrared light with wavelength 700–1000 nm could transport through tissue with scattering-limited attenuation and minimal heating [25]. Hence, to make the nanoplates purer and smaller, the long-wavelength SPR band blue shift to below 1000 nm will be very helpful in allowing gold nanoplates to be suitable for more practical applications.

Here we bring forward a convenient approach to size-controlled gold nanoplates based on a modified seed-mediated, iodide ion (I^-)- and cetyltrimethylammonium bromide (CTABr)-assisted synthetic system [26]. In current research, the edge size of the as-generated nanoplates can be easily tuned from 140 to 30 nm by adjusting the quantity of seeds and I^-, without changing the thickness or crystal structure of the nanoplates, and accordingly moving the long-wavelength SPR peak from 1055 to 750 nm. Moreover, we have developed a facile strategy to achieve these gold nanoplates to a high purity by taking advantages of the quite different electrostatic aggregation effects between nanoplates and spherical nanoparticles. Effective storage methods to keep the structural and optical stability of these gold nanoplates are also proposed.

2. Experimental details

CTABr was purchased from Sigma (cat. No: H6269, which contains negligible iodide [27]). $HAuCl_4$, sodium citrate, $NaBH_4$, KI, L-ascorbic acid, NaOH, and NaCl were all purchased from Shanghai Sinopharm Chemical Reagent Co. Ltd (China). All reagents were used as-received. All the glassware was cleaned by aqua regia and Millipore-quality water; (18.2 MΩ cm) was used throughout the experiments. Briefly, the gold nanoplates were prepared by a seed-mediated growth approach. The seeds were obtained by 0.5 ml $NaBH_4$ (ice-cold, 0.1 M) reducing 0.2 ml $HAuCl_4$ (25 mM) in the surroundings of 40 ml sodium citrate (250 μM) solution and kept at 25 °C for 2 h. Then, the nanoplates were formed when the seeds were added to a growth solution which was prepared by adding 0.5 ml $HAuCl_4$ (25 mM), 27.5 μl KI (0.1 M), 275 μlL-ascorbic acid (0.1 M), and 275 μl NaOH (0.1 M) to a 50 ml CTABr (0.025 M) solution. After 3 h, NaCl was added to raise the sum of [Cl^-] and [Br^-] up to 0.2 M. After another 3 h, the purple reaction solution mainly containing spherical gold nanoparticles was poured out and water was added to the container, then the gold nanoplates deposited from the reaction solution and clinging to the container were redispersed to form a stable colloidal solution. In total, this quantity of reagents was abbreviated '1×'. To correspondingly increase the amount of seeds and I^- would have resulted in smaller nanoplates. The smaller the nanoplates are, the more NaCl is needed to raise the sum of [Cl^-] and [Br^-] up to a higher level. Subsequent preparing additions were referred to as 2×, , 3×, 5×, and 10× seeds and I^-, with the amount of seeds and I^- correspondingly increased to 2, 3, 5, 10 times while the other reagents were equivalent to those described for 1×.

The resulting gold nanostructures were characterized by transmission electron microscopy (TEM) (JEM-2000EX, JEOL) operating at 120 kV. High resolution TEM (HRTEM) images and selected area electron diffraction (SAED) patterns were characterized by a JEOL JEM-2100 transmission electron microscope operating at 200 kV. Ultraviolet–visible–near-infrared (UV–vis–NIR) absorption spectra of the samples were recorded by a UNICO 2802S spectrophotometer with wavelength ranging from 300 to 1100 nm.

3. Results and discussion

Figure 1(a) shows a digital photograph and UV–vis–NIR absorption spectrum of the as-collected gold nanoplates with 1× seeds and I^-. It can be observed clearly in the spectrum that there is no peak at 500–600 nm, indicating very few spherical gold nanoparticles in the suspension [28]. From the spectrum, we can also identify the in-plate dipole and quadrupole plasmon resonances of the gold nanoplates. It should be noted that these two plasmon resonances (quadrupole and dipole) are not distinguishable from one another with spherical particles; however, in anisotropic particles such as nanoplates, these two plasmon resonances oscillate markedly differently (generally separated by 100–400 nm), and can be demonstrated experimentally for nanoplates of both gold and silver [8]. The green color of the suspension is mostly due to the absorption band caused by quadrupole plasmon resonances (around 760 nm) and can be explained by analyzing the spectrum, which indicates low absorption at the green wavelengths (500–570 nm) and increased absorption at the red wavelengths (610–780 nm). The green transparent suspension is also strong evidence that there is no large sized side product and very few spherical nanoparticles. There is an intensive absorption peak around 1055 nm caused by the in-plate dipole plasmon resonances, which is useful in near-infrared absorption applications. The two absorption bands are both similar to the previous report [23], but are enhanced thanks to the high purity. The TEM image reveals the shape triangle nanoplate with edge lengths 140 ± 25 and 8 ± 2 nm in thickness, while very few side products are observed (figure 1(b)). Figure 1(c) shows the corresponding HRTEM image, from which we can recognize that the nanoplates are single-crystal. The fringes with a spacing of 0.25 nm correspond to the forbidden 1/3{422} reflections [29], and these fringes extend across the entire plate. As can be seen in figure 1(d), which reveals the SAED pattern of the nanoplates, there is a hexagonal diffraction spot array corresponding to a

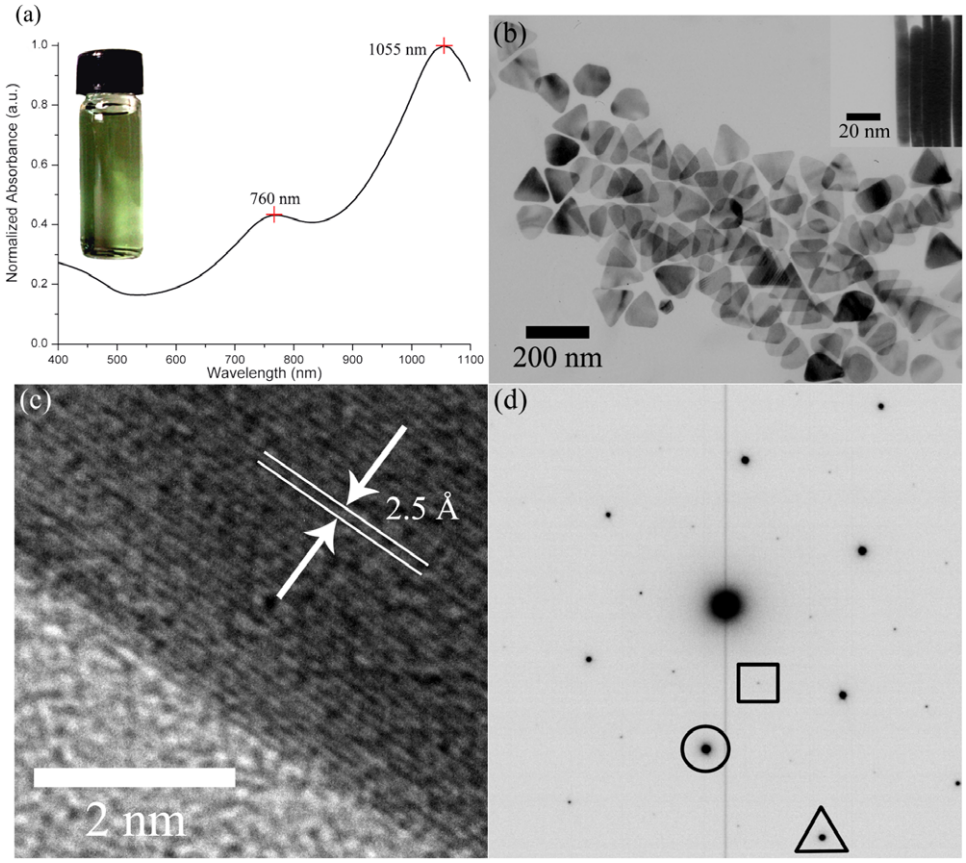

Figure 1. (a) UV–vis–NIR spectrum, (b) TEM images, (c) HRTEM image, and (d) SAED pattern of the redispersed gold nanoplates using 1× seeds and I^-. The inset in panel (a) shows a digital photograph of the gold nanoplates. The inset in panel (b) shows a TEM image of a stack of the gold nanoplates. The spots in (d) marked by a box, circle, and triangle correspond to 1/3{422}, {220}, and {422} diffractions, respectively.

single crystal with an atomically flat surface. The spot marked by a box corresponds to 1/3{422} diffraction, whose presence has demonstrated the existence of stacking faults parallel to the {111} surface extending across the entire plate [23].

We have adjusted the gold nanoplates to be smaller by simply increasing the amount of gold seeds and I^- in the reaction solution. The resulting nanostructures can be collected and redispersed similarly to those adding 1× seeds and I^- except when 10× seeds and I^- are added in our experiments. Since there was no precipitation observed after in NaCl when adding 10× seeds and I^-, we centrifuged the supernate and redispersed the pellet as resulting products in this control. Figure 2 shows digital photos and UV–vis–NIR absorption spectra of the size-controlled nanostructures which added 2×, 3×, 5×, 10× seeds, and I^-. As can be seen in the spectra, the absorption peak can be adjusted to 532 nm. Although the enhanced optical absorption bands can also be contributed by nanoparticle agglomerates [30, 31], nanoplates hold the characteristics as a kind of monodisperse nanoparticle, thus enabling more potential applications in the solution phase and *in vivo*. The easily tunable spectra will also benefit from more usages such as multiplex detection [32]. The relatively narrow size distribution suggests their good monodispersity. Figures 3(a)–(c) and (g) show a series of TEM images of the corresponding nanostructures from adding 2×, 3×, 5×, 10× seeds, and I^-. It can be seen that the structures are nanoplates with edge lengths 70 ± 15 nm, 50 ± 12 nm, 30 ± 10 nm, and spherical nanoparticles with diameter 30 ± 2 nm, respectively. The nanostructures remain triangular nanoplates when adding no more than 5× seeds and I^-, but they tend to form spherical nanostructures when adding 10× seeds and I^-. As shown in figure 3(d)–(f), the thickness of the nanoplates with different edge lengths is almost the same (8 ± 2 nm). Figure 3(h) shows the corresponding HRTEM image of the nanoplates adding 5× seeds and I^-, from which we can see the single-crystal structure and fringes with a spacing of 0.25 nm extending across the entire plate corresponding to the forbidden 1/3{422} reflections [23]. This demonstrates that the gold nanoplates can be adjusted consecutively from 140 to 30 nm without changing their crystal structure.

It should be noticed that the seeds are prepared using sodium citrate as stabilizer rather than using CTABr. The main reason is that the seeds prepared by this approach mostly have stacking faults, which is helpful to obtain plate-like nanostructures [33]. Figure 3(i) shows a TEM image of the resulting nanostructures when no I^- is added to the reaction solution, from which the twinned plane can be observed clearly. It provides strong evidence that the seeds have stacking faults across the entire particles. Another key to obtain gold nanoplates lies in the I^-. As reported by Ha *et al* [26], halide ions (Cl^-, Br^-, and I^-) often play important roles during the seed-mediated growth of gold nanoparticles in a

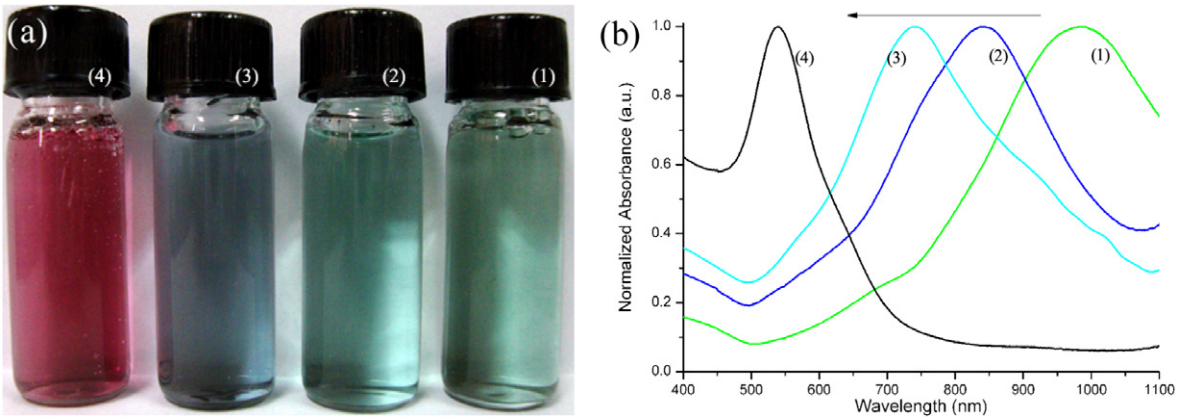

Figure 2. (a) Digital photograph and (b) UV–vis–NIR spectra of the resulting gold nanostructures adding (1) 2×, (2) 3×, (3) 5×, and (4) 10× seeds and I^-.

system employing CTABr as cationic surfactant. In our control experiments, we have repeated the preparing process without adding I^-. The observed nanostructures are twinned nanorices and nanorods along the ⟨011⟩ direction, as shown in figure 3(i). This indicates that I^- plays a decisive role in suppressing {111} facets, leaving other facets absorbing more gold atoms and growing much faster, the same as in previous reports [26]. Therefore, when more seeds are added to form more growing points in the size-control process, we need to add more I^-, too.

As a kind of two-dimensional nanostructure, nanoplates, compared with spherical nanoparticles, have a much larger contact area between each other. Thus they need more repulsion force to keep them stable in suspension. Figure 4 shows the status of the repulsion force of the nanoplates in different growth periods. When the ion concentration of the solution is higher, anions electrostatically absorb to the CTA^+ bilayers on the surface of the nanoplates, and their negative charge neutralizes the positive charge of part of CTA^+. As a result, the repulsion force between nanoplates caused by CTA^+ decreases. Thus, the nanoplates aggregate and are deposited at the bottom of the reaction container while the spherical nanoparticles are still in the solution. After redispersion, the ion concentration decreases again, inducing the repulsion force between the nanoplates recovered, and high-purity colloidal gold nanoplates are obtained at last. Smaller nanoplates need less repulsion force to keep their stability and more ions are needed to make them deposit. On the other hand, the CTA^+ bilayers densely cover on gold nanoplates and their space blocking effect makes the plates remain isolated and monodisperse [34]. Hence, the nanoplates can be collected and redispersed easily to form a colloidal suspension due to the recovery effects of the CTA^+ bilayer. Please note that in our strategy we have added NaCl to increase the ion concentration instead of adding more CTABr. This is firstly because there is already much CTABr in the solution, we cannot add so much more CTABr before it saturates. Another reason is that CTABr, while in high concentration, is easy to subject to crystallization when the temperature decreases. Moreover, NaCl is non-toxic and much cheaper.

A possible mechanism of the size-control process is depicted in figure 5. In seed-mediated synthetic procedures, the seeds are added to the growth solution to serve as growing points. Then atoms generated by the metal precursor are absorbed on these seeds to form metal nanostructures rather than generating new growing points. When more seeds are added in our synthetic system (shown by the second row in figure 5), more growing points are formed. But the number of free gold atoms generated by the invariable amount of $HAuCl_4$ is still unchanged. Thus, fewer gold atoms deposit on each seeds. Without enough supply of gold atoms, the seeds grow to smaller nanoplates. The smaller nanoplates can also be sent to the bottom of the container by proper amounts of ions following the possible mechanism described in figure 4. On the other hand, since I^- is a key point to suppress {111} facets and is conducive to the growth of nanoplates, more I^- are needed to cover the increased {111} facets area when the number of seeds increases. With enough I^-, the growth of {111} facets is greatly restrained and other facets of the gold nanostructures grow much faster than the {111} facets. As a result, the gold nanostructure forms a nanoplate and grows up to a certain size which depends on the number of gold atoms in the solution. As a contrast, we added 2× and 3× seeds in the reaction solution without adding more I^-. As can be observed from the absorption spectra shown in figure 6(a), the size distribution becomes much wider when more seeds are added. This indicates the loss of monodispersity of the resulting nanostructures and the key point of I^- in obtaining plate-like nanostructures. We have done another control experiment by adding more I^- without adding more seeds. Figure 6(b) shows the absorption spectra of adding 2× seeds, with 2×, 10×, and 20 × I^-, respectively. It is clearly revealed that even when 20 × I^- are added, the absorption peaks are still beyond 800 nm. This is proof that the approach of adding more seeds with correspondingly more I^- to size-control the high-purity colloidal gold nanoplates is more effective.

The proper amount of CTABr can protect the shape of the nanoplates well and enhance the stability of the colloidal solution. As a demonstration, we centrifuged the redispersed suspension several times, and dispersed it in water. Then, there was no free CTABr in the solution, and some of the CTA^+ bilayer absorbed on the nanoplates dissociated. After 30 min, the absorption peak of the gold nanoplates blue

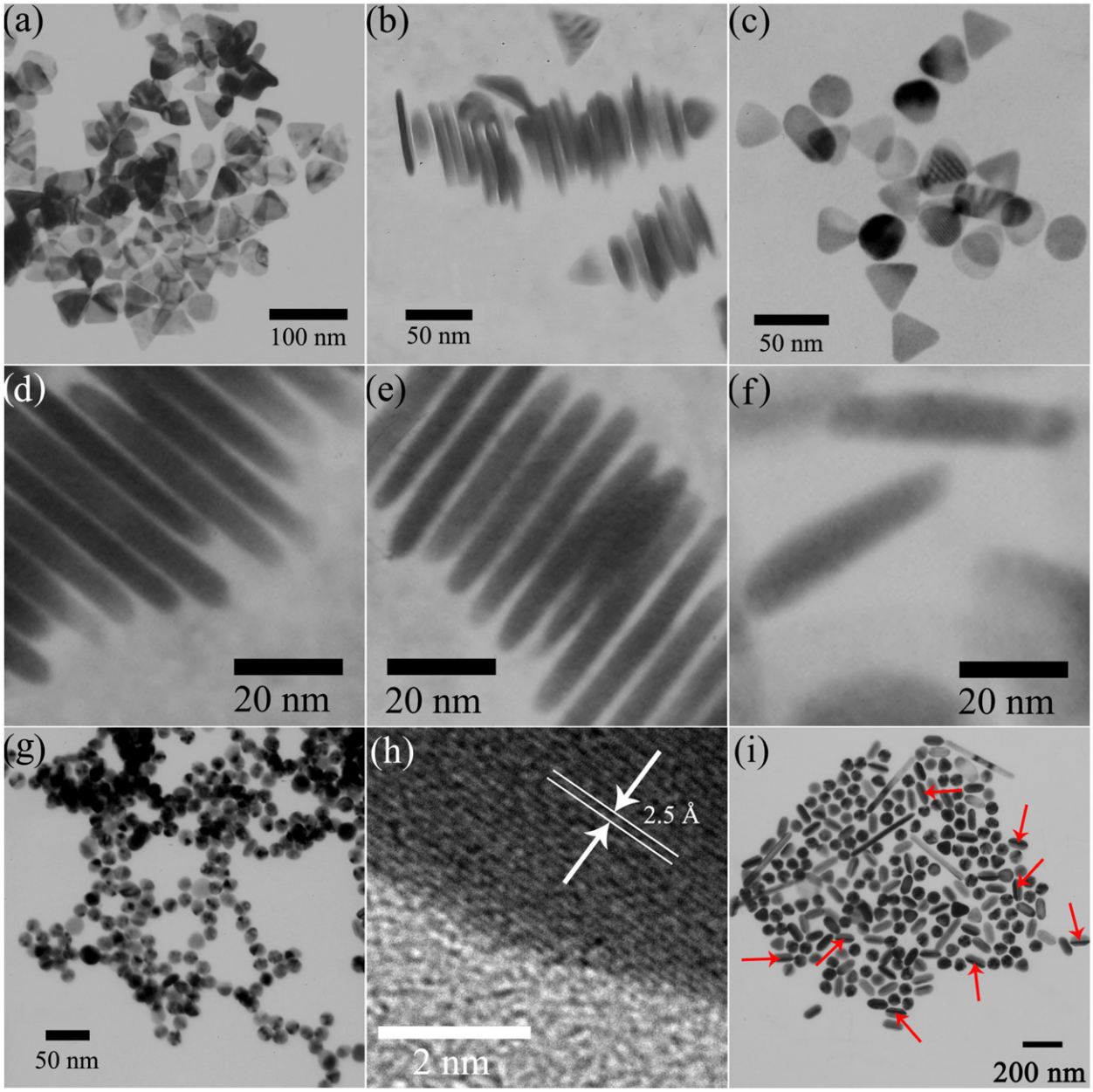

Figure 3. TEM images of the resulting gold nanostructures adding (a) 2×, (b) 3×, (c) 5×, and (g) 10× seeds and I^-, and stacked gold nanoplates adding (d) 2×, (e) 3×, and (f) 5× seeds and I^-, respectively. (h) HRTEM of the gold nanoplates adding 5× seeds and I^-. (i) TEM image of the gold nanostructures obtained without adding any I^-. The red arrows point to several stacking faults.

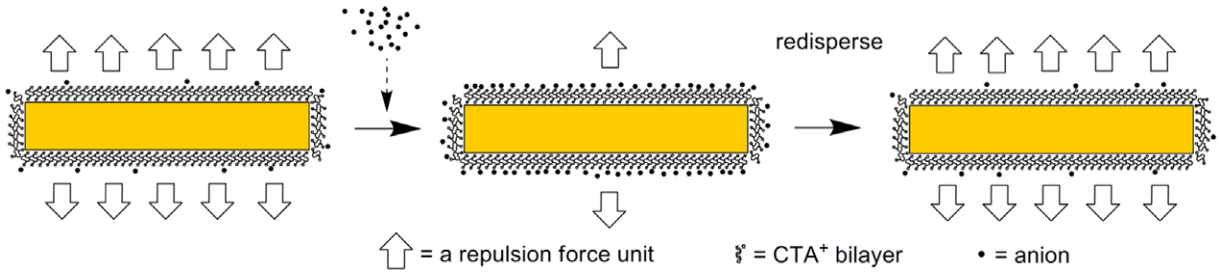

Figure 4. Schematic of grown, deposited, and redispersed gold nanoplates. A hollow arrow represents a repulsion force unit caused by electrostatic repulsion. More hollow arrows around the nanoplates means more repulsion force which mainly depends on the positive charge of the CTA^+ bilayer subtracting the negative charge of anions binding to the nanoplates.

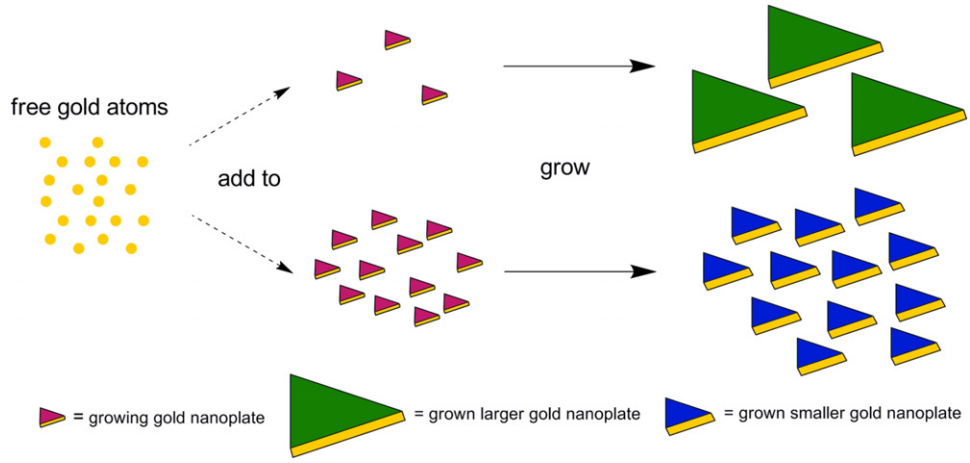

Figure 5. Schematic of the size-control process. The number of free gold atoms is a constant. If there are more seeds in the reaction solution, the number of gold atoms adding to each seed decreases. As a result, smaller gold nanoplates are produced.

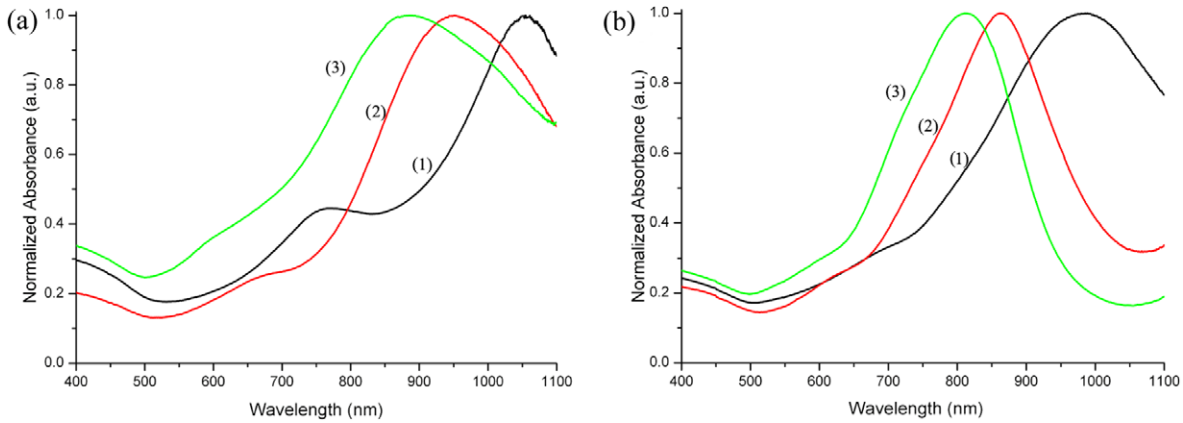

Figure 6. (a) UV–vis–NIR spectra of the gold nanostructures adding 1 × I^-, with (1) 1×, (2) 2×, (3) 3× seeds, respectively. (b) UV–vis–NIR spectra of the gold nanostructures adding 2× seeds, with (1) 2×, (2) 10×, (3) 20 × I^-, respectively.

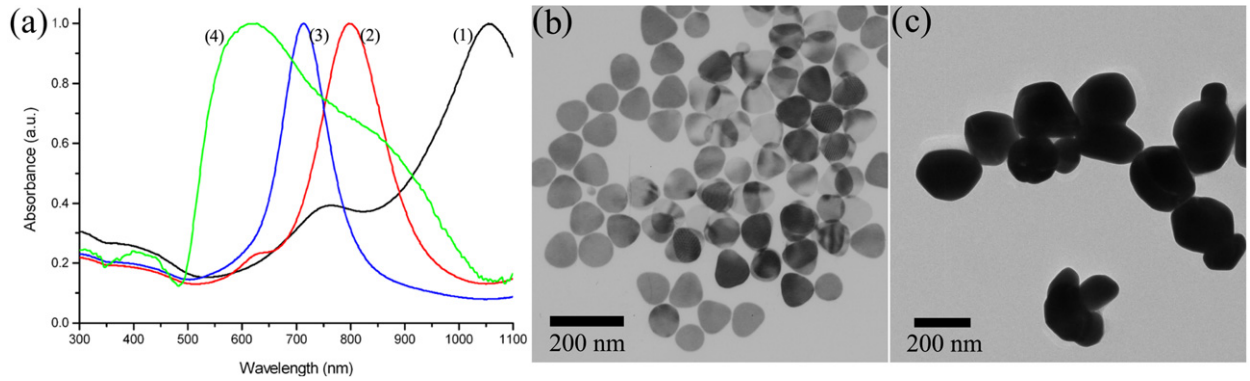

Figure 7. (a) UV–vis–NIR spectra of the gold nanostructures purified from CTABr and allowed to sit for (1) 0 min, (2) 30 min, (3) 6 h, and (4) 72 h, respectively. TEM images of the gold nanostructures obtained after sitting for (b) 6 h, and (c) 72 h, respectively.

shifted to ∼800 nm. As time went on, the absorption peak continued blue shifting. 72 h later, the absorption peak further blue shifted to ∼600 nm with decrease of monodispersity (figure 7(a)). We can also observe the change of shape in the TEM images (figures 7(b) and (c)). The shape turns to disk-like nanoplates and then large spherical structures which are more stable in thermodynamics. Furthermore, we have worked out effective storage methods for the gold nanoplates as follows. Briefly, the grown and deposited gold nanoplates can be kept as precipitates without pouring out the supernate for weeks. When the precipitation was redispersed, the gold nanoplate suspension can be stored stably for months

in a 5 mM CTABr aqueous solution. Moreover, a suitable coating such as polyelectrolyte will allow the well-stored gold nanoplates to have versatile uses if necessary.

4. Conclusion

In summary, we have demonstrated a facile while flexible strategy to obtain colloidal gold nanoplates, and successfully adjust their edge lengths consecutively from 140 to 30 nm to better fit potential applications. Moreover, we achieved their high-purity colloidal solution by taking advantage of the interface-dependent electrostatic aggregation effects. Also, we investigated the possible mechanism of crystal growth and size-control of these gold nanoplates and developed effective storage methods. Although the monodispersity of the smaller gold nanoplates obtained by this method was a little decreased, it is believed that properly adjusting the amount of reactants will lead to better results in the future. In addition, these high-purity colloidal gold nanoplates, with a large flat surface and strong near-infrared absorption, enable them to be a class of suitable nano-platforms for cancer hyperthermia, drug delivery, and controlled release.

Acknowledgments

This work was supported by the National Basic Research Program of China (2006CB933206), the National Natural Science Foundation of China (NSFC, 60725101, 30870679, 30970787), and the China Postdoctoral Science Foundation (20090451236).

References

[1] Yavuz M S, Jensen G C, Penaloza D P, Seery T A P, Pendergraph S A, Rusling J F and Sotzing G A 2009 *Langmuir* **25** 13120
[2] Herle P S, Ellis B, Coombs N and Nazar L F 2004 *Nat. Mater.* **3** 147
[3] Jeong S, Woo K, Kim D, Lim S, Kim J S, Shin H, Xia Y and Moon J 2008 *Adv. Funct. Mater.* **18** 679
[4] Lewis L N 1993 *Chem. Rev.* **93** 2693
[5] Somorjai G A 1996 *Chem. Rev.* **96** 1223
[6] El-Sayed M A 2001 *Acc. Chem. Res.* **34** 257
[7] Xia Y, Xiong Y J, Lim B and Skrabalak S E 2009 *Angew. Chem. Int. Edn* **48** 60
[8] Millstone J E, Hurst S J, Metraux G S, Cutler J I and Mirkin C A 2009 *Small* **5** 646
[9] Maillard M, Giorgio S and Pileni M P 2003 *J. Phys. Chem.* B **107** 2466
[10] Qin L D, Zou S L, Xue C, Atkinson A, Schatz G C and Mirkin C A 2006 *Proc. Natl. Acad. Sci. USA* **103** 13300
[11] Loo C, Lowery A, Halas N, West J and Drezek R 2005 *Nano Lett.* **5** 709
[12] Chen J *et al* 2005 *Nano Lett.* **5** 473
[13] Schmid G 1992 *Chem. Rev.* **92** 1709
[14] Jin R, Cao Y C, Hao E, Metraux G S, Schatz G C and Mirkin C A 2003 *Nature* **425** 487
[15] Xue C and Mirkin C A 2007 *Angew. Chem. Int. Edn* **46** 2036
[16] Ghosh P, Han G, De M, Kim C K and Rotello V M 2008 *Adv. Drug Deliv. Rev.* **60** 1307
[17] Qian X M *et al* 2008 *Nat. Biotechnol.* **26** 83
[18] Shankar S S, Rai A, Ankamwar B, Singh A, Ahmad A and Sastry M 2004 *Nat. Mater.* **3** 482
[19] Sun X P, Dong S J and Wang E 2004 *Angew. Chem.-Int. Edn* **43** 6360
[20] Guo Z R, Zhang Y, Huang L, Wang M, Wang J, Sun J F, Xu L N and Gu N 2007 *J. Colloid Interface Sci.* **309** 518
[21] Guo Z R, Zhang Y, Xu A Q, Wang M, Huang L, Xu K and Gu N 2008 *J. Phys. Chem.* C **112** 12638
[22] Ah C S, Yun Y J, Park H J, Kim W J, Ha D H and Yun W S 2005 *Chem. Mater.* **17** 5558
[23] Goy-Lopez S, Castro E, Taboada P and Mosquera V 2008 *Langmuir* **24** 13186
[24] Millstone J E, Metraux G S and Mirkin C A 2006 *Adv. Funct. Mater.* **16** 1209
[25] Hirsch L R, Stafford R J, Bankson J A, Sershen S R, Rivera B, Price R E, Hazle J D, Halas N J and West J L 2003 *Proc. Natl. Acad. Sci.* **100** 13549
[26] Ha T H, Koo H J and Chung B H 2007 *J. Phys. Chem.* C **111** 1123
[27] Smith D K, Miller N R and Korgel B A 2009 *Langmuir* **25** 9518
[28] Njoki P N, Lim I I S, Mott D, Park H Y, Khan B, Mishra S, Sujakumar R, Luo J and Zhong C J 2007 *J. Phys. Chem.* C **111** 14664
[29] Kirkland A I, Jefferson D A, Duff D G, Edwards P P, Gamesons I, Johnson B F G and Smith D 1993 *Proc. R. Soc.* A **440** 589
[30] Khriachtchev L, Heikkila L and Kuusela T 2001 *Appl. Phys. Lett.* **78** 1994
[31] Zhang J, Li Q, Di X W, Liu Z L and Xu G 2008 *Nanotechnology* **19** 435606
[32] Yu C X and Irudayaraj J 2007 *Anal. Chem.* **79** 572
[33] Liu M Z and Guyot-Sionnest P 2005 *J. Phys. Chem.* B **109** 22192
[34] Sethi M, Joung G E and Knecht M R 2009 *Langmuir* **25** 317